Biomimetic Synthesis of Macroscopic-Scale Calcium Carbonate Thin Films. Evidence for a Multistep Assembly Process

Guofeng Xu,[#,†] Nan Yao,[†] Ilhan A. Aksay,[†,§] and John T. Groves*[,#,†]

Contribution from the Departments of Chemistry and Chemical Engineering and the Princeton Materials Institute, Princeton University, Princeton, New Jersey 08544

Received June 1, 1998

Abstract: Biologically controlled mineralization features an orchestrated balance among various controlling factors such as spatial delineation, template promotion, crystal growth modification and cessation, and so on. Highly ordered calcium carbonate lamellae formed in the nacreous layers of mollusk (aragonite), the foliated calcitic layers of mollusk (calcite), or the semi-nacre of brachiopods (calcite) are excellent examples of the outcome of such synergistic control. Mimicking the concerted interplay of template promotion and growth inhibition as often utilized in biomineralization, we have synthesized macroscopic and continuous calcium carbonate thin films with thickness ranging from 0.4 to 0.6 μm. The thin films were prepared at air/subphase interfaces by promoting mineral deposition with amphiphilic porphyrin templates, coupled with growth inhibition by the use of poly(acrylic acid) as a soluble inhibitor. Films formed at 22 °C were found to have a biphasic structure containing both amorphous and crystalline calcium carbonate. The crystalline regions were identified to be calcite oriented with the (00.1) face parallel to the porphyrin monolayer at the air/subphase interface. Films obtained in the early stage of formation at lower temperature (4 °C) displayed characteristics of a single amorphous phase. These observations suggest that films formed through a multistage assembly process, during which an initial amorphous deposition was followed by a phase transformation into the ultimate crystalline phase and the orientation of the crystalline phase was controlled by the porphyrin template during the phase transformation. The results provide new insights into the template-inhibitor−biomineral interaction and a new mechanism for synthesizing ceramic thin film under mild conditions.

Introduction

Applications for ceramic thin films are demanding new synthetic methods which can exert more precise control over both the microscopic and the macroscopic structure of films under mild conditions.[1−3] Traditional technologies that involve high-temperature or high-vacuum processing are inadequate for this purpose, especially in systems where high temperatures cannot be tolerated.[2,4] There have been increasing recent efforts in search of innovative biomimetic processing strategies to produce inorganic thin films.[3,4] The majority of these efforts have focused on exploring the promoting effect of templates on crystal nucleation and growth.[5−7] Several categories of such approaches can be discerned, according to the nature and structural complexity of the templates employed.

The first approach focuses on the in vitro[8−14] or *in vivo*[15−18] functions of the biological matrix. These investigations have yielded valuable information on how matrix proteins can affect biomineral formation. However, due to their formidable structural complexity, much work is yet to be done to illustrate the nature of these biological systems.

The second approach uses synthetic polymeric analogues as substrates for the deposition of polycrystalline inorganic materials:[19] Thus, calcium carbonate has been deposited on model

* To whom correspondence should be addressed.
[#] Department of Chemistry.
[§] Department of Chemical Engineering.
[†] Princeton Materials Institute.

(1) (a) Aksay, I. A.; Trau, M.; Manne, S.; Honma, I.; Yao, N.; Zhou, L.; Fenter, P.; Eisenberger, P. M.; Gruner, S. M. *Science* **1996**, *273*, 892−898. (b) Moya, J. S. *Adv. Mater.* **1995**, *7*, 185−189. (c) Manne, S.; Aksay, I. A. *Curr. Opin. Solid State Mater. Sci.* **1997**, *2*, 358−364. (d) Mann, S. *J. Mater. Chem.* **1995**, *5*, 935−946.

(2) Lange, F. F. *Science* **1996**, *273*, 903.

(3) Heuer, A. H.; Fink, D. J.; Laraia, V. J.; Arias, J. L.; Calvert, P. D.; Kendall, K.; Messing, G. L.; Blackwell, J.; Rieke, P. C.; Thompson, D. H.; Wheeler, A. P.; Veis, A.; Caplan, A. I. *Science* **1992**, *255*, 1098.

(4) Bunker, B. C.; Rieke, P. C.; Tarasevich, B. J.; Campbell, A. A.; Fryxell, G. E.; Graff, G. L.; Song, L.; Liu, J.; Virden, J. W.; McVay, G. L. *Science* **1994**, *264*, 48.

(5) Berman, A.; Ahn, D. J.; Lio, A.; Salmeron, M.; Reichert, A.; Charych, D. *Science* **1995**, *269*, 515.

(6) Addadi, L.; Moradian, J.; Shay, E.; Maroudas, N. G.; Weiner, S. *Proc. Natl. Acad. Sci. U.S.A.* **1987**, *84*, 2732.

(7) Heywood, B. R.; Rajam, S.; Mann, S. *J. Chem. Soc., Faraday Trans.* **1991**, *87*, 727.

(8) Greenfield, E. M.; Wilson, D. C.; Crenshaw, M. A. *Am. Zool.* **1984**, *24*, 925.

(9) Wheeler, A. P.; Sikes, C. S. *Am. Zool.* **1984**, *24*, 933.

(10) Addadi, L.; Weiner, S. *Proc. Natl. Acad. Sci. U.S.A.* **1985**, *82*, 4110.

(11) Albeck, S.; Aizenberg, J.; Addadi, L.; Weiner, S. *J. Am. Chem. Soc.* **1993**, *115*, 11691.

(12) Falini, G.; Albeck, S.; Weiner, S.; Addadi, L. *Science* **1996**, *271*, 67.

(13) Belcher, A. M.; Wu, X. H.; Christensen, R. J.; Hansma, P. K.; Stucky, G. D.; Morse, D. E. *Nature* **1996**, *381*, 56.

(14) Shenton, W.; Pum, D.; Sleytr, U. B.; Mann, S. *Nature* **1997**, *389*, 585.

(15) Fritz, M.; Belcher, A. M.; Radmacher, M.; Walters, D. A.; Hansma, P. K.; Stucky, G. D.; Morse, D. E.; Mann, S. *Nature* **1994**, *371*, 49.

(16) Zaremba, C. M.; Belcher, A. M.; Fritz, M.; Li, Y.; Mann, S.; Hansma, P.; Morse, D. E.; Speck, J. S.; Stucky, G. D. *Chem. Mater.* **1996**, *8*, 679.

(17) Schaffer, T. E.; Ionescu-Zanetti, C.; Proksch, R.; Fritz, M.; Walters, D. A.; Almqvist, N.; Zaremba, C. M.; Belcher, A. M.; Smith, B. L.; Stucky, G. D.; Morse, D. E.; Hansma, P. K. *Chem. Mater.* **1997**, *9*, 1731.

(18) Levi, Y.; Albeck, S.; Brack, A.; Weiner, S.; Addadi, L. *Chem. Eur. J.* **1998**, *4*, 389.

(19) Calvert, P.; Rieke, P. *Chem. Mater.* **1996**, *8*, 1715.

10.1021/ja9819108 CCC: $15.00
Published on Web 11/10/1998

polymeric substrates[6,20] and even inorganic polymer surfaces;[21] iron oxides and tin oxide were deposited on sulfonated polystyrene films;[4,22] cadmium sulfide and titanium oxide were assembled on absorbed polyelectrolyte surfaces;[23] and hydroxyapatite was also deposited on polymers.[24,25] A major problem with this method is that the macromolecule surface is usually too rough and complicated to allow an understanding of the interfacial interactions at a molecular level. Consequently, it is very difficult to achieve precise control over mineralization by such routes.

The third approach has made use of the well-ordered two-dimensional structure of a self-assembled film on a solid substrate or a Langmuir film at the air/water interface as the nucleating template.[26] Calcium carbonate,[7] iron oxides,[27] cadmium or zinc sulfide,[23] hydroxyapatite,[28] and more recently zirconium oxides[29] have been grown under such amphiphilic monolayers. Though this method has provided important insight into the relationships between the structure of the substrate and the overgrowing crystals,[5,30] most amphiphiles used seem to be structurally too fluid to simulate the biogenic control exhibited by natural matrix proteins. Moreover, under such conditions, only discrete crystals rather than continuous films were formed.

A recent approach has employed synthetic supramolecular assemblies to offer semirigid templates for calcium carbonate crystallization.[31,32] For example, we have demonstrated that the function of the acidic glycoprotein matrix could be mimicked in vitro with a supramolecular assembly of porphyrin amphiphiles.[31]

None of the approaches so far have exerted control over the mineral growth in the direction perpendicular to the template with respect to parallel deposition. To produce an extended two-dimensional structure, lateral growth should be favored over normal growth. A template alone is apparently insufficient to fulfill this requirement. Nature, on the other hand, has offered many examples of minerals forming well-ordered thin-film structures, even for brittle materials such as calcium carbonate. Highly oriented aragonite tablets are found in the molluscan nacreous layers. Ordered to a less extent but highly laminated as well are calcitic thin layers existing in both the foliated calcite layers of mollusk[33,34] and the semi-nacre of brachiopods.[34−36] Although different detailed mechanisms have been proposed for the growth and orientation of these thin laminar structures,[8,9,17,37−39] a controlled inhibition of mineral growth, either by generating preformed organic compartment or by episodically releasing inhibitive organic substances, has been a common feature. Clearly, the interplay of mineral growth initiation and cessation, administered by the interlaminar organic matrix, has played a critical role in determining the two-dimensional structure with a controlled thickness.

Various acidic proteins extracted from biological minerals have shown the remarkable ability to inhibit crystal growth or to modify crystal habit.[40,41] In different extracts, both specific and nonspecific protein−mineral interface interactions have been identified. On the basis of specific interactions, small molecules[42] or small peptides[43] have been "tailor-made" to affect crystal morphology by inhibiting the growth of particular crystal faces. Synthetic anionic polypeptide analogues[44] and anionic non-peptide polymers[45] have also been found to be potent inhibitors or habit modifiers of inorganic crystallization, via a similar mechanism by adsorption onto the surfaces of the growing crystals, thus controlling their growth rate and habit through the strength and selectivity of this adsorption.[3,46] Poly(acrylic acid), for example, is well-known to prevent calcium carbonate from scaling.[47]

We have sought to design model organic templates of moderate and understandable structural complexity that can mimic the function of matrix proteins in promoting crystallization. As mentioned earlier, we have recently employed am-

(20) Zhang, S.; Gonsalves, K. E. *J. Appl. Polym. Sci.* **1995**, *56*, 687.
(21) Wong, K. K. W.; Brisdon, B. J.; Heywood, B. R.; Hodson, A. G. W.; Mann, S. *J. Mater. Chem.* **1994**, *4*, 1387.
(22) Tarasevich, B. J.; Rieke, P. C.; Liu, J. *Chem. Mater.* **1996**, *8*, 292.
(23) Fendler, J. H.; Meldrum, F. C. *Adv. Mater.* **1995**, *7*, 607.
(24) Dalas, E.; Kallitsis, J.; Koutsoukos, P. G. *Langmuir* **1991**, *7*, 1822.
(25) Kokubo, T. *Eur. J. Solid State Inorg. Chem.* **1995**, *32*, 819.
(26) For the nucleation and crystal growth of organic crystals beneath monolayer films, see the following references: (a) Landau, E. M.; Levanon, M.; Leiserowitz, L.; Lahav, M.; Sagiv, J. *Nature* **1985**, *318*, 353. (b) Landau, E. M.; Wolf, G.; Levanon, M.; Leiserowitz, L.; Lahav, M.; Sagiv, J. *J. Am. Chem. Soc.* **1989**, *111*, 1436. (c) Popovitz-Biro, R.; Wang, J. L.; Majewski, J.; Shavit, E.; Leiserowitz, L.; Lahav, M. *J. Am. Chem. Soc.* **1994**, *116*, 1179. (d) Weissbuch, I.; Berkovic, G.; Yam, R.; Als-Nielson, J.; Kjaer, K.; Lahav, M.; Leiserowitz, L. *J. Phys. Chem.* **1995**, *99*, 6036. (e) Cooper, S. J.; Sessions, R. B.; Lubetkin, S. D. *J. Am. Chem. Soc.* **1998**, *120*, 2090.
(27) Rieke, P. C.; Tarasevich, B. J.; Wood, L. L.; Engelhard, M. H.; Baer, D. R.; Fryxell, G. E. *Langmuir* **1994**, *10*, 619.
(28) Lin, H.; Yanagi, T.; Seo, W. S.; Kuwabara, K.; Koumoto, K. *Phosphorus Res. Bull.* **1996**, *6*, 39.
(29) Agarwal, M.; DeGuire, M. R.; Heuer, A. H. *J. Am. Ceram. Soc.* **1997**, *80*, 2967.
(30) Lochhead, M. J.; Letellier, S. R.; Vogel, V. *J. Phys. Chem. B* **1997**, *101*, 10821.
(31) Lahiri, J.; Xu, G.; Dabbs, D. M.; Yao, N.; Aksay, I. A.; Groves, J. T. *J. Am. Chem. Soc.* **1997**, *119*, 5449.
(32) Litvin, A. L.; Valiyaveettil, S.; Kapaln, D.; Mann, S. *Adv. Mater.* **1997**, *9*, 124.
(33) Runnegar, B. *Alcheringa* **1984**, *8*, 273.
(34) Lowenstam, H. A.; Weiner, S. *On Biomineralization*, 1st ed.; Oxford University Press: New York, 1989.
(35) Armstrong, J. D. *J. Geo. Soc. Aust.* **1970**, *17*, 13.
(36) Weedon, M. J.; Taylor, P. D. *Biol. Bull.* **1995**, *188*, 281.
(37) Watabe, N. In *Inorganic biological crystal growth*; Pamplin, B. R., Ed.; Pergamon Press: New York, 1981.
(38) Wheeler, A. P.; George, J. W.; Evans, C. A. *Science* **1981**, *212*, 1397.
(39) Sikes, C. S.; Wheeler, A. P. *Biomineralization and biological metal accumulation*; Westbroek, P., de Jong, E. W., Eds.; Reidel Publishing: Holland, 1983.
(40) (a) Berman, A.; Addadi, L.; Weiner, S. *Nature* **1988**, *331*, 546−548. (b) Gunthorpe, M. E. *Biol. Bull.* **1990**, *179*, 191−200. (c) Wheeler, A. P.; Low, K. C.; Sikes, C. S. In *Surface reactive peptides and polymers*; Sikes, C. S., Wheeler, A. P., Eds.; American Chemical Society: Washington, DC, 1991. (d) Wada, N.; Okazaki, M.; Tachikawa, S. *J. Cryst. Growth* **1993**, *132*, 115−121. (e) Burgess, S.; Oxendine, S. L. *J. Protein Chem.* **1995**, *14*, 655−664.
(41) Aizenberg, J.; Hanson, J.; Koetzle, T. F.; Weiner, S.; Addadi, L. *J. Am. Chem. Soc.* **1997**, *119*, 881.
(42) (a) Berkovitch-Yellin, Z.; Van Mil, J.; Addadi, L.; Idelson, M.; Lahav, M.; Leiserowitz, L. *J. Am. Chem. Soc.* **1985**, *107*, 3111−22. (b) Addadi, L.; Berkovitch-Yellin, Z.; Weissbuch, I.; van, M. J.; Shimon, L. J. W.; Lahav, M.; Leiserowitz, L. *Angew. Chem., Int. Ed. Engl.* **1985**, *24*, 466−485. (c) Davey, R. J.; Black, S. N.; Bromley, L. A.; Cottier, D.; Dobbs, B.; Rout, J. E. *Nature* **1991**, *353*, 549−550. (d) Mann, S.; Didymus, J. M.; Sanderson, N. P.; Heywood, B. R. *J. Chem. Soc., Faraday Trans.* **1990**, *86*, 1873−1880.
(43) DeOliveira, D. B.; Laursen, R. A. *J. Am. Chem. Soc.* **1997**, *119*, 10627.
(44) (a) Sikes, C. S.; Yeung, M. L.; Wheeler, A. P. In *Surface reactive peptides and polymers*; Sikes, C. S., Wheeler, A. P., Eds.; American Chemical Society: Washington, DC, 1991. (b) Wierzbicki, A.; Sikes, C. S.; Madura, J. D.; Drake, B. *Calcif. Tissue Int.* **1994**, *54*, 133−141. (c) Sims, S. D.; Didymus, J. M.; Mann, S. *J. Chem. Soc., Chem. Commun.* **1995**, 1031−1032.
(45) (a) Falini, G.; Gazzano, M.; Ripamonti, A. *J. Cryst. Growth* **1994**, *137*, 577−584. (b) Didymus, J. M.; Oliver, P.; Mann, S.; DeVries, A. L.; Hauschka, P. V.; Westbroek, P. *J. Chem. Soc., Faraday Trans.* **1993**, *89*, 2891−2900. (c) Manne, J. S.; Biala, N.; Smith, A. D.; Gryte, C. C. *J. Cryst. Growth* **1990**, *100*, 627−634.
(46) (a) Furedi-Milhofer, H.; Sarig, S. *Prog. Cryst. Growth Charact.* **1996**, *32*, 45−74. (b) Gratz, A. J.; Hillner, P. E. *J. Cryst. Growth* **1993**, *129*, 789−793.
(47) (a) Sekine, I.; Sanbongi, M.; Hagiuda, H.; Oshibe, T.; Yuasa, M.; Imahama, T.; Shibata, Y.; Wake, T. *J. Electrochem. Soc.* **1992**, *139*, 3167−3173. (b) Okubo, T.; Mohri, N. *Macromolecules* **1988**, *21*, 2744−2747. (c) Hudson, A. P.; Woodward, F. E.; McGrew, G. T. *J. Am. Oil Chem. Soc.* **1988**, *65*, 1353−1356.

phiphilic anionic porphyrins at the air/water interface as a template for biomimetic calcite formation.[31] The calcite crystals thus obtained bore similar features (e.g. morphology and orientation) to those nucleated by acidic glycoprotein matrix in vitro.[10,11] Here, we describe the syntheses of macroscopic and continuous calcium carbonate thin films at a porphyrin template/subphase interface by employing poly(acrylic acid) as a soluble inhibitor to mimic the cooperative promotion−inhibition in biogenic thin film production.[48] The strategy is to prevent crystal growth in the direction normal to the template so as to limit the space available for mineral growth to the very thin layer right below the promoting substrate. The forced two-dimensional growth then leads to the formation of continuous thin films.

More significantly, we observed a phase transformation process from an initially deposited amorphous phase to crystalline calcite during the film formation. The lattice orientation of the crystals was found to be controlled by the porphyrin template in the course of this phase transformation, providing direct evidence for a multistep deposition and crystallization process in this biomimetic model system. This sequence of events stands in contrast to the prevailing view that nuclei form as crystalline particles directly,[49,50] but it is analogous to processes known to be utilized by organisms.[51,52]

Results

A semirigid template for crystallization was spontaneously formed via the self-organization of the amphiphilic tricarboxyphenylporphyrin iron(III) μ-oxo dimer (**1**) at an air/$Ca(HCO_3)_2$ solution interface as we have described.[31] The formation of the porphyrin template did not require compression and solidlike domains were spontaneously generated due to the intermolecular interactions between the porphyrin amphiphiles, even at submonolayer coverage.[53] This observation is consistent with the isothermal behavior of **1** at the air/subphase interface (Figure 1). During the compression of the film, a sharp transition from an expanded state to a condensed state occurred without other intermediates, indicating a coalescing process of preformed domains. Each porphyrin molecule was determined to occupy 56−58 Å^2 over the calcium bicarbonate subphase, corresponding to a nearly vertical orientation of the porphyrin plane at the interface.[31] Calcite crystals that were formed under this porphyrin template were oriented with the (00.1) face parallel to the template, as we have previously shown.[31]

In the presence of 20−30 ppm poly(acrylic acid) inhibitor, a slowed mineralization process yielded a large and readily visible thin film that spanned an area of several square centimeters.[54] When viewed from above, the film looked slightly yellow-green, a color similar to that of the porphyrin monolayer. When viewed from an angle, the film appeared iridescent, suggesting that the thickness of the film was comparable to the wavelength

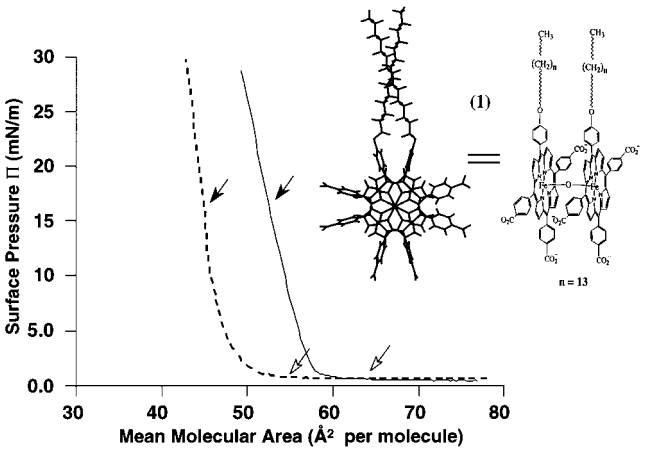

Figure 1. The surface pressure (Π) vs mean molecular area isotherm and the molecular structure of the amphiphilic tricarboxyphenylporphyrin iron(III) μ-oxo dimer (**1**). The mean molecular area occupied by each porphyrin dimer was measured from the isotherms at 25 °C to be 112−116 and 92−96 Å^2 over saturated calcium bicarbonate solution (solid line) and deionized water (dashed line), respectively. The open arrows indicate the liquid expanded state regions and the solid arrows indicate the condensed state regions.

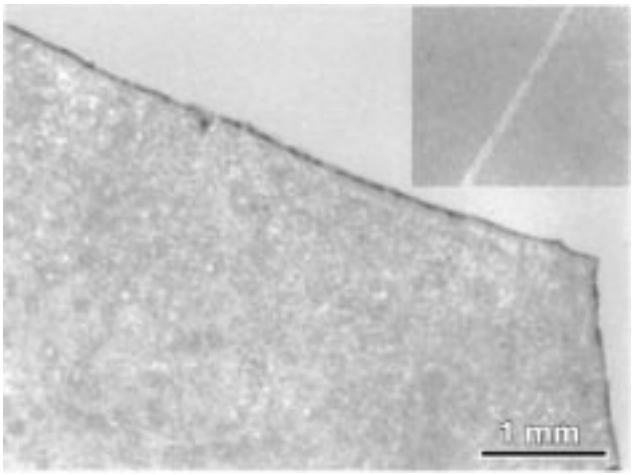

Figure 2. An optical micrograph of the calcium carbonate thin film picked up and dried on a cover-glass slide. Inset: An in situ optical micrograph of the same thin film at the air/water interface. The stripe running from the lower left to the upper right in the inset is a crack introduced into the film mechanically to contrast the blank air/water interface.

of the visible light (0.4−0.8 μm). When viewed with the optical microscope under cross-polarized light, the appearance of the film did not change with the rotation of the polarizer, indicating a macroscopically uniform structure and the absence of macroscopic crystalline objects. In situ optical microscopy showed the film as a thin, transparent, smooth, and continuous sheet (Figure 2 inset). The stripe cutting through the center of the image is a crack mechanically introduced into the film to contrast it with the blank subphase surface. The film could be deposited easily on various substrates. After being picked up and dried in the air, the film appeared flat and transparent (Figure 2); some areas of the film, however, tended to crack and curl upon drying (Figure 3c inset).

Under the scanning electron microscope (SEM), the two sides of the film were strikingly different (Figure 3a). One side was rough while the other side was smooth. Based upon the deposition method used, the smooth side corresponded to the side facing the porphyrin monolayer and the rough side

(48) A template/inhibition strategy for the synthesis of $CaCO_3$ thin film has been employed independently: Kato, T.; Suzuki, T.; Amamiya, T.; Irie, T.; Komiyama, M.; Yui, H. at Nanostructured Materials in Biological and Artificial Systems−The 11th Toyota Conference, Mikkabi, Shizuoka, Japan, November, 1997, Personal communication.

(49) *Biomineralization: chemical and biological perspectives*; Mann, S., Webb, J., Williams, J. P., Eds.; VCH: New York, 1989.

(50) Heywood, B. R.; Mann, S. *Chem. Mater.* **1994**, *6*, 311.

(51) Lowenstam, H. A.; Weiner, S. *Science* **1985**, *227*, 51.

(52) Beniash, E.; Aizenberg, J.; Addadi, L.; Weiner, S. *Proc. R. Soc. London B* **1997**, *264*, 461.

(53) Kroon, J. M.; Sudholter, E. J. R.; Schenning, A. P. H. J.; Nolte, R. J. M. *Langmuir* **1995**, *11*, 214.

(54) A small number of three-demensional flowerlike crystals were observed in some regions close to the edges of the trough.

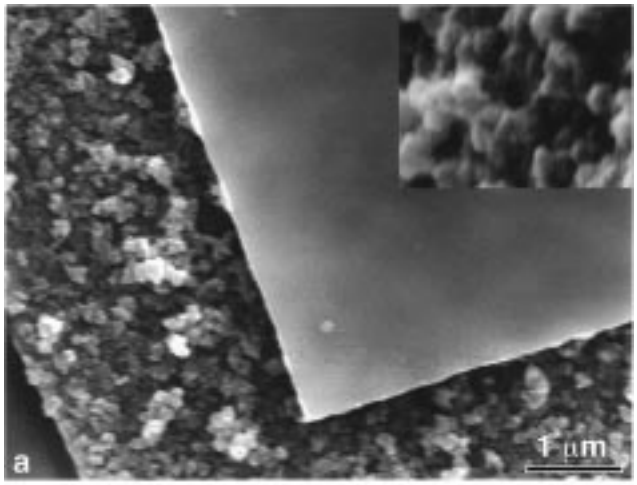

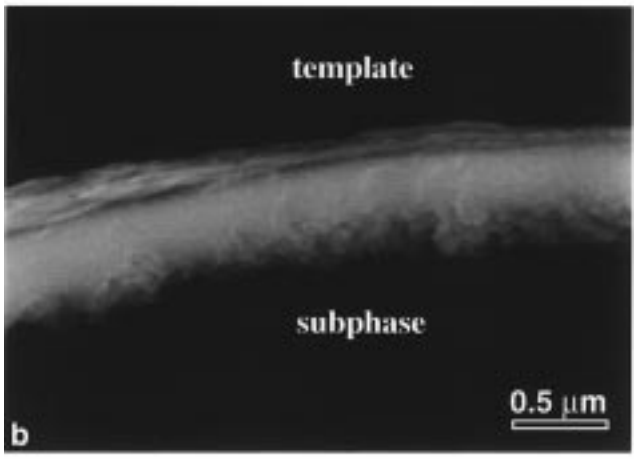

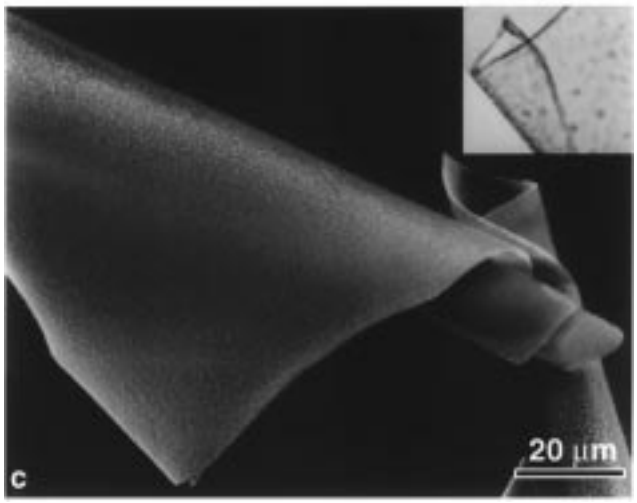

Figure 3. Scanning electron microscope images of calcium carbonate thin films. (a) One piece of film was placed on top of another, allowing a view of two different sides of the film simultaneously. The smooth side was facing the template and the rough and particulate side was facing the subphase. The inset shows the rough side at higher magnification. (b) A cross-sectional view of the film and its orientation relative to the template and the subphase. (c) Films that curved after being dried on hydrophobic silicon wafer. The inset is the optical micrograph of the curved film.

corresponded to the growth front in the solution. The rough side was covered with numerous particles (ca. 100 nm) that showed considerable intergrowth (Figure 3a inset). By contrast, the smooth side appeared flat and featureless even at higher

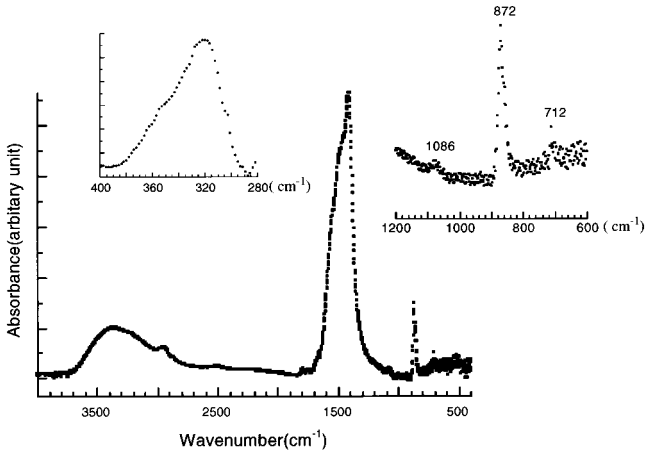

Figure 4. FTIR spectra of the calcium carbonate thin film picked up and dried.

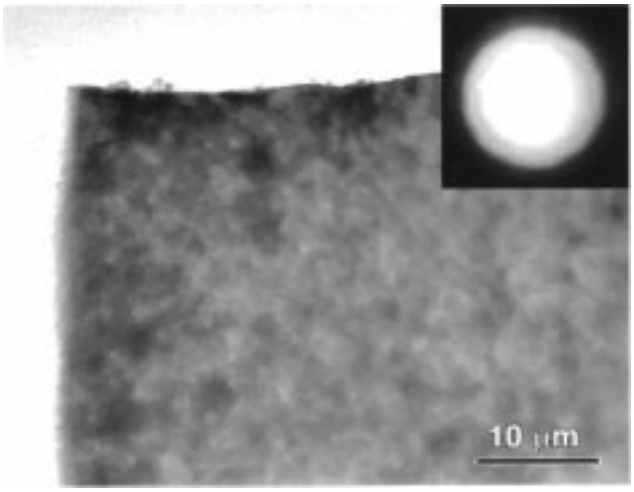

Figure 5. A bright field TEM image of the calcium carbonate film at low magnification. The inset is the electron diffraction pattern from the film.

magnification. A view of the cross section of the film observed by tilting the sample stage showed that the region close to the smooth side was condensed and the region close to the rough side was more particulate (Figure 3b). Measurements taken at different sites from different segments of the film yielded a uniform film thickness of 0.4 μm with a deviation less than 10%, indicating a continuous and homogeneous growth. Depending upon the experimental conditions such as temperature, inhibitor concentration, and the time period allowed for film growth, the thickness of different films could range from 0.4 to 0.6 μm, which is coincidentally similar to that of the calcite laminae formed by many organisms.[33,35,36]

Some regions of the film examined with SEM also appeared highly curled (Figure 3c), similar to what was observed with the optical microscope. This tensile property of the film is in sharp contrast to the brittle nature of crystalline calcium carbonate, implying either the inclusion of organic material or the presence of a large amount of amorphous phase. To determine the amount of organic content within the film, air-dried film was analyzed by thermogravimetric analysis and differential scanning calorimetry (TGA/DSC). Two weight loss regimes were observed as the film was heated from 25 to 900 °C in the air flow. About 10% weight loss first occurred at 440 °C, which was attributed to the decomposition of the organic component in the film since pure polyacrylate was found to decompose at the same temperature. Based on the area of the

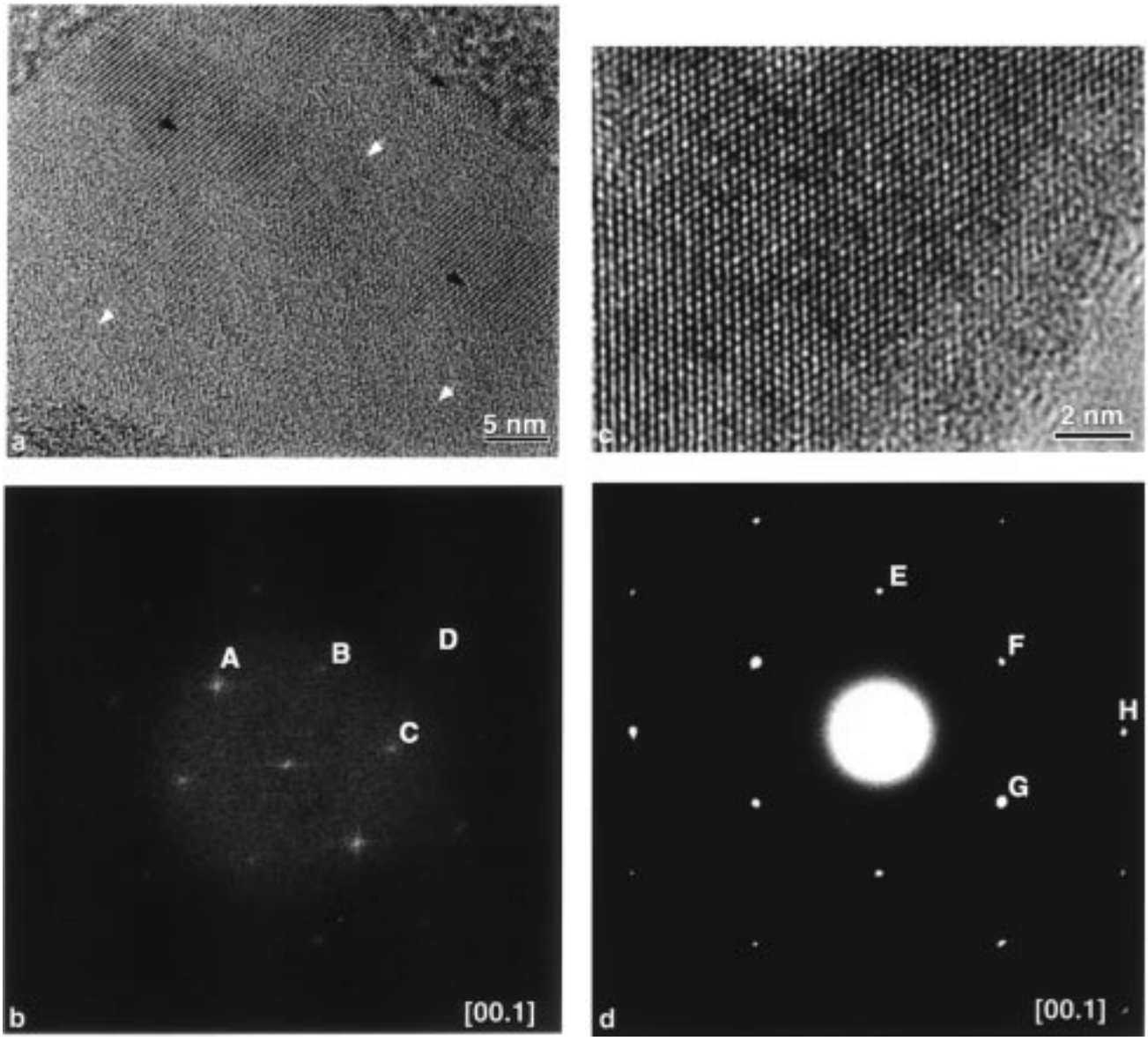

Figure 6. (a) High resolution transmission electron microscope (HRTEM) image of a partially crystallized area in the calcium carbonate film. Crystalline domains (black arrows) scattered in the amorphous phase matrix (white arrows) and some disorder existed within the crystalline region. The image plane was perpendicular to the [00.1] zone axis of a pseudohexagonal calcite lattice. The separation between two neighboring fringes was about 4.33 Å, corresponding to the *d* spacing of the calcite {10.0} plane. The image was taken from the fractured edge of a film, at close to Scherzer defocus condition. (b) A digital electron diffraction pattern obtained from the lattice image in (a) with the program DigitalMicrograph 2.5. The pattern was a slightly distorted hexagon: A (−11.0), B (01.0), C (10.0), and D (11.0). (c) HRTEM image of a crystallographically mature region of the film. The image plane was also perpendicular to the [00.1] zone axis of the hexagonal calcite lattice. The fringe spacing (ca.. 2.49 Å) corresponded to that of the {11.0} plane. (d) Select area electron diffraction pattern from the crystalline film in (c), showing a perfect hexagonal pattern: E (−12.0), F (11.0), G (2−1.0), and H (30.0). The image was taken under similar conditions as (a).

film picked up for the thermal analysis and the mean molecular area of the porphyrin molecule, the amount of porphyrin affiliated with the film was estimated to be around to 3 wt %, assuming a full monolayer coverage. A second and final weight loss of the film started at 580 °C and ended at 680 °C, which we attribute to the decomposition of $CaCO_3$. However, since this temperature range is significantly lower than that of the decomposition of commercial polycrystalline calcium carbonate powder (630−720 °C), we suggest the existence of metastable amorphous calcium carbonate.

The mineralogy of the film was also characterized by FT-IR spectroscopy (Figure 4). A strong absorption occurring around 1414 cm^{-1} was characteristic of calcium carbonate. Simultaneous occurrence of absorption peaks at 872, 712, and 320 cm^{-1} indicated the presence of crystalline calcite.[52,55] However, the absorption was much weaker at 712 cm^{-1} than at 872 cm^{-1}. The 712 and 872 cm^{-1} peaks were assigned to the υ_4 and υ_2 absorption bands of CO_3^{2-} in calcite, respectively, and their intensity ratio ($I_{max}\upsilon_2/I_{max}\upsilon_4$) has been used to diagnose the coexistence of calcite and amorphous calcium carbonate:[52] a higher $I_{max}\upsilon_2/I_{max}\upsilon_4$ ratio corresponds to a higher content of amorphous carbonate. In the present case, this ratio is about 4.3. Since the ratio ($I_{max}\upsilon_2/I_{max}\upsilon_4$) of pure calcite was reported as ca. 3.0,[52] our results suggested the film contained both crystalline and amorphous phases. In addition, the occurrence of a small but diffuse peak at 1086 cm^{-1} and the broadening of the peaks around 3340 cm^{-1} were also indicative of the presence of an amorphous phase.[56,57] This observation was reinforced

(55) *Infrared transmission spectra of carbonate minerals*, 1st ed.; Jones, G. C., Jackson, B., Eds.; Chapman & Hall: London, 1993.

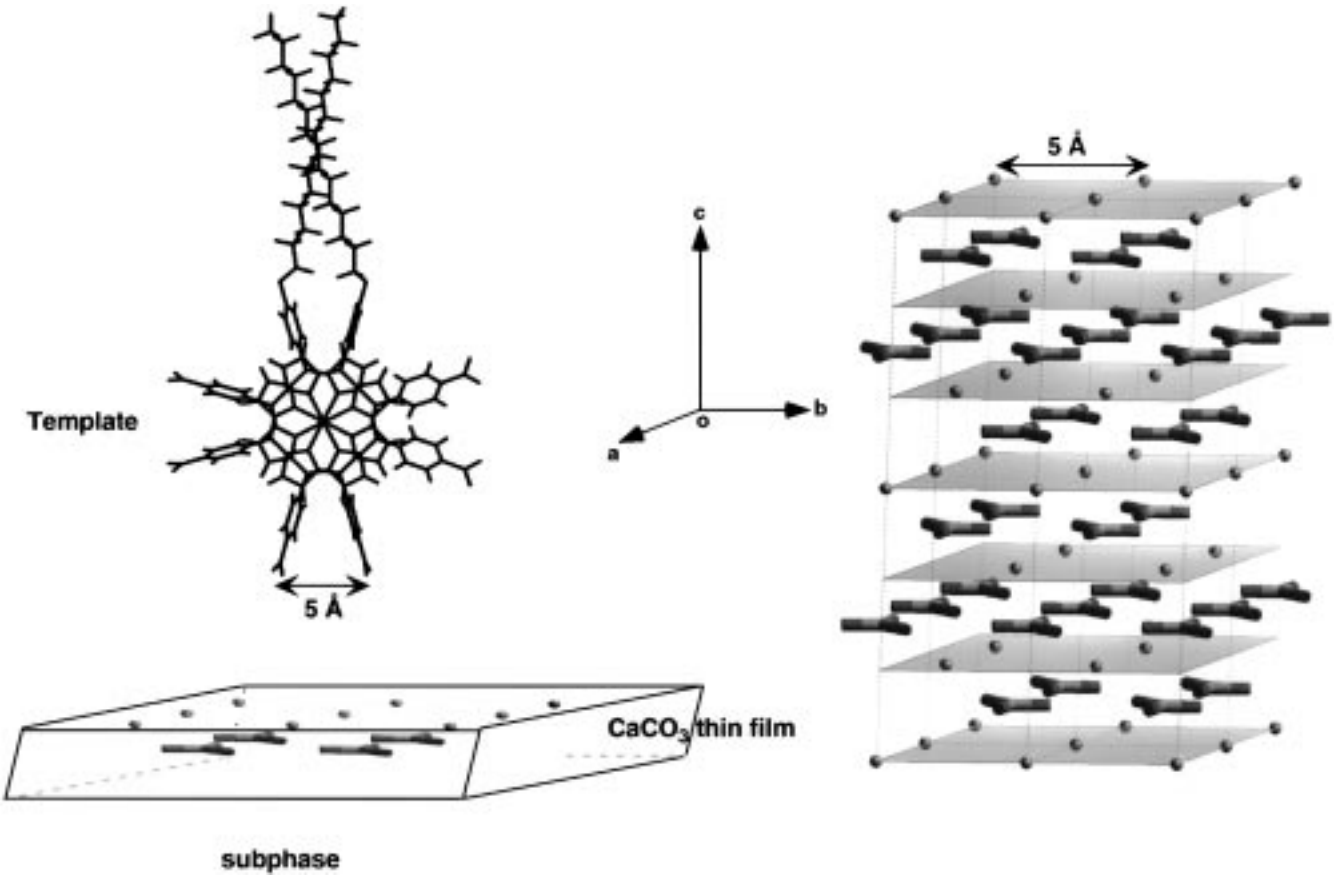

Figure 7. A graphic representation of the relative orientation of the film, the crystal axes, the calcite (00.1) plane, the template and the subphase (left), and a ball-cylinder model of the calcite crystal lattice generated by Cerius2. The spheres represent calcium cations and the triangular cylinders represent carbonate anions.

by transmission electron microscopy (TEM) bright field imaging and electron diffraction, which showed a very diffuse ring pattern typical of a mixture of amorphous and crystalline phase (Figure 5). The presence of both the calcite and amorphous calcium carbonate phases in the film is highly suggestive of a phase transformation from the latter to the former.[52]

To determine the structure and the orientation of the crystalline phase, we performed high resolution transmission electron microscopy (HRTEM) on the films. HRTEM images were taken from the edge of fractured films and low dose electron beam was used to avoid possible damage to the samples. Under these experiment conditions, the samples were stable. The extent of crystallization across the film was inhomogeneous, with some regions being more crystallographically mature than others. In those partially crystallized regions, scattered crystalline domains were imbedded in the amorphous phase matrix (Figure 6a). The crystal patches were determined to be calcite based on the *d* spacing value (ca. 4.33 Å) of the lattice fringes which corresponded to the interplanar distance of the {10.0} plane and the hexagonal digital electron diffraction pattern obtained from the image (Figure 6b). The appearance of the {10.0} plane is unusual since it is forbidden by symmetry in a perfect hexagonal calcite lattice. Instead, it is the {30.0} plane that normally appears. However, a closer examination of the electron diffraction from the film revealed that the pattern deviated slightly from that of a perfect hexagon (Figure 6b). Computer modeling with the Cerius2 program showed that when slight distortions were introduced into the normal calcite hexagonal lattice, a pseudohexagonal pattern of {10.0} diffraction appeared as a result of symmetry breaking. This observation supports the conjecture that a phase transformation from amorphous to a crystalline phase occurs, especially at the initial stage when the domain size is very small. Further confirmation came by examining the larger and more mature crystalline regions where the fringes of the {11.0} instead of the {10.0} plane were prevalent (Figure 6c). The electron diffraction from the same area produced a perfect hexagonal pattern, which contained reciprocal lattice points from both the {11.0} and the {30.0} planes but not the {10.0} plane (Figure 6d).

Interestingly, the hexagonal diffraction patterns obtained above indicate that the orientation of the crystalline areas in both cases is the same (Figures 6b and 6d). That is, the calcite {00.1} plane was parallel to the film and hence, the porphyrin template (Figure 7), the same orientation as the calcite crystals formed under the same porphyrin template in the absence of the inhibitor.[31] By contrast, crystals formed without the porphyrin template oriented randomly both in the presence and in the absence of the inhibitor. These observations indicate that the control of crystal orientation, though occurring at a later time, is staged by the porphyrin template during the phase transformation.[58]

(56) Aizenberg, J.; Lambert, G.; Adadi, L.; Weiner, S. *Adv. Mater.* **1996**, *8*, 222.

(57) Brecevic, L.; Nielsen, A. E. *J. Cryst. Growth* **1989**, *98*, 504.

(58) The semicrystalline film could stay stable for about 60 h. Prolonged settlement would lead to the overgrowth of crystalline phase at the expense of the amorphous phase. The crystalline film thus obtained was thicker and brittle and lost preferential orientation as determined from X-ray diffraction pattern. This is likely due to the interaction of PAA with the developing crystalline domain, which results in the modification of the crystal orientation and growth.

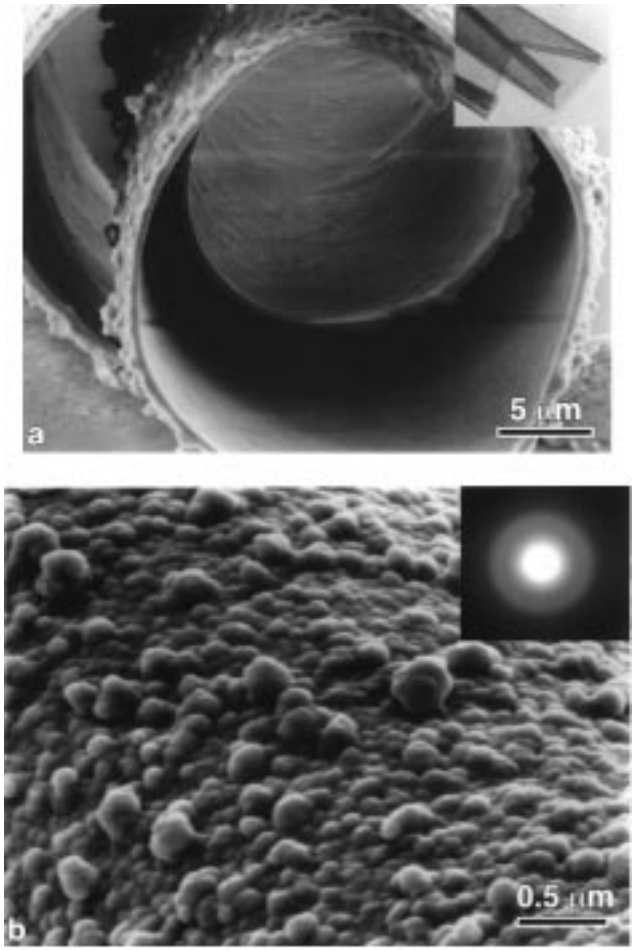

Figure 8. (a) SEM micrograph of the film synthesized at 4 °C, picked up and dried on a glass slide. The inset is an optical micrograph of a similar film. (b) High magnification SEM image of the film showing the rough side that faced the subphase. The inset shows the electron diffraction pattern of the film by TEM.

To further verify this phase transformation mechanism, we conducted similar experiments at low temperature (4 °C) at which the amorphous calcium carbonate was both thermodynamically and kinetically more stable.[57,59] We anticipated that this procedure would allow the capture of the pure amorphous phase before the phase transformation had taken place. Compared with the room temperature experiments, the growth of films at 4 °C was significantly slower. After 3−4 weeks, the films that formed appeared macroscopically similar to the films grown at room temperature. Films thus obtained were more flexible and readily curled into rolls when being picked up and air-dried. The two opposite sides of the film also differed distinctively from each other, a very smooth side facing the porphyrin template and a rough side facing the subphase (Figure 8). However, FTIR spectra of these films lacked the υ_4 peak (712 cm^{-1}) compared with those of room temperature films, indicating the absence of crystalline calcite. Indeed, the electron diffraction from the low-temperature films confirmed that they were entirely amorphous (Figure 8b inset). These amorphous films were stable under the experimental conditions and no irradiation-induced crystalline phase formation was observed. After being kept in a desiccator at room temperature for several months, the same sample stayed amorphous. Prolonged settlement of the films at the air/subphase interface could however lead to calcite formation as determined by X-ray diffraction studies. These results reassured us of the initial deposition of the amorphous precursor phase that subsequently transformed into the ordered crystalline phase (Scheme 2).

(59) (a) Clarkson, J.; Price, T. J.; Adams, C. J. *J. Chem. Soc., Faraday Trans.* **1992**, *88*, 243−249. (b) Ogino, T.; Suzuki, T.; Sawada, K. *Geochim. Cosmochim. Acta* **1987**, *51*, 2757−2767.

Scheme 1. A Schematic Representation of the Experimental Setup for Preparing $CaCO_3$ Thin Films at the Interface of the Air/Aqueous Subphase[a]

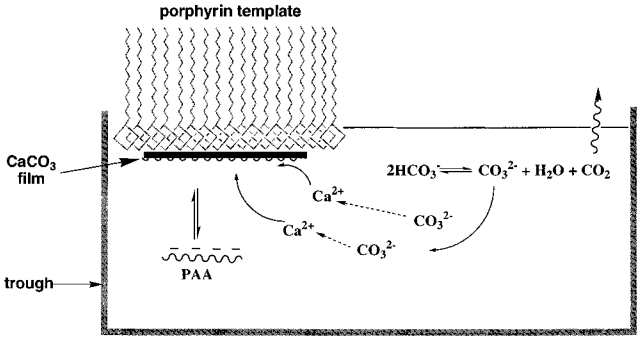

[a] The surface pressure of the porphyrin template was about 20 mN/m, corresponding to a solid-like monolayer. The porphyrin monolayer was not compressed by the barrier, and the whole setup was left undisturbed in a temperature-constant environment during the film formation.

Discussion

It is commonly accepted that the protein matrix plays a very important role in regulating biomineral formation. However, there remain many unknowns as to how the matrix affects the crystallization process, especially the initial nucleation. In general, the formation of certain mineral phases can proceed through two pathways. A crystal could precipitate via epitaxy directly from the liquid solution so that the nuclei bear the same structure as the final crystal. Alternatively, the final crystalline phase could arise through a series of steps, initiated by the formation of an amorphous phase that undergoes subsequent phase transformations. In this case, the structure of the initial solid material would be much different from that of the final crystal. The traditional view of epitaxy emphasizes the structural similarity between the matrix and the assumed nucleating crystal face, implying a direct crystallization process. Consequently, this leads to the belief that the matrix controls the crystallization from the very beginning. Although there are some observations that could be explained by this mechanism,[6,10] strong and direct evidence for such a process is lacking.

On the other hand, a multistep crystallization process may be plausible, especially in a biological environment in which temporal modifications of the crystallization kinetics may be prevalent. Dissection of the crystallization process into several stages could make the activation energy of each step lower than that of the one-step precipitation. Since the initial phase formed under conditions of sequential precipitation would be the most soluble phase, a lower energy barrier is expected according to the Ostward−Lussac law.[60] The existence of several phases would enable organisms to control mineralization through intervention with the kinetics. By selectively interacting with the mineral at different stages during the crystal forming process, the organisms could choose to manipulate both the polymorph and the orientation of the mineral to meet specific biological requirements. Given the great diversity in the phase, morphol-

(60) (a) Mann, S. *Struct. Bonding* (*54*): *Inorganic elements in biochemistry*; Springer-Verlag: New York, 1983. (b) Leadbeater, B.; Riding, R., Eds. *Biomineralization in lower plants and animals*; Clarendon Press: New York, 1986.

Scheme 2. A Schematic Comparison between the Direct Epitaxy Path (Open Arrow) and the Multistep Phase Transformation Path (Solid Arrows)

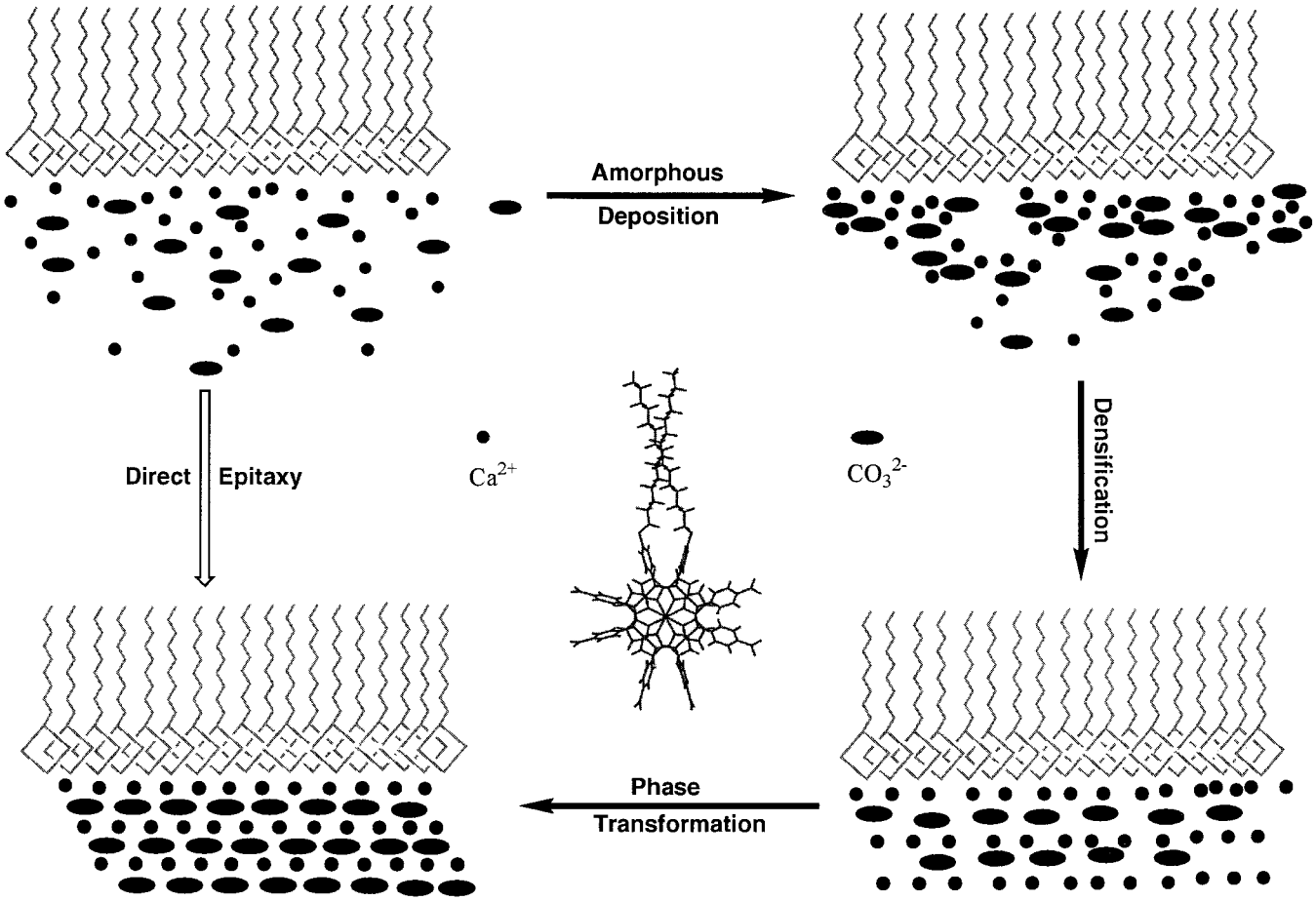

ogy, and orientation of biominerals, the likelihood for complicated multistep crystallization mechanisms seems high.

Important experimental evidence for multistep crystallization should include detection of amorphous phases and subsequent phase transformation. Since the amorphous phase is more soluble than the stable crystalline phase, it should be the first solid phase formed during the crystallization and therefore could be prevalent in biomineralization.[60] In fact, amorphous phase minerals have been identified in many organisms.[61] Recently, Addadi and Weiner et al. have suggested that amorphous calcium carbonate may be much more widespread than commonly supposed in biology, but has been overlooked because of the difficulty of identifying an amorphous phase in the presence of a crystalline phase of the same composition.[52,56] Transformations from the amorphous to the crystalline phase have also been discovered and characterized in several cases of biological mineralization.[51,52] The phase transformation observed in the thin film formation in our laboratories has therefore provided direct evidence in a model system for a multistep crystallization process that can be an important alternative pathway for biological mineralization.

During the phase transformation, the porphyrin template played significant roles. Although it is not yet possible to quantitize the individual function, several structural features of this porphyrin monolayer must be involved in the template's regulation. First, the porphyrin monolayer offers a semirigid template. Certain structural rigidity is required for biological templates to function as a nucleation template. For example, acidic glycoproteins could nucleate calcium carbonate crystallization only when immobilized by an insoluble matrix such as chitin.[34] Second, the porphyrin monolayer offers a pure negatively charged surface that compensates the pure positively charged (00.1) face of calcite. The calcite (00.1) face is made up of alternating layers of calcium cations and carbonate anions; each layer is either positively or negatively charged (Figure 7). This type of crystal plane is usually unstable because of high interfacial energy associated with the surface charge. However, the nucleation of the calcite at the (00.1) face is found in nature, and many calcite-bearing organisms adopt an orientation such that the (00.1) face is aligned parallel to an acidic protein template.[50,62] Thus, the expression of the calcite (00.1) face is regarded as biogenicly relevant.[6,10,11] Third, the carboxylate arrays afforded by the porphyrin template provide adjustable structural definition. There is a close match between the Ca−Ca distance in the calcite (00.1) face and the intercarboxylate distance in the porphyrin dimer (Figure 7), according to the molecular modeling.[31] In the meantime, the porphyrin template allows certain flexibility for structure adjustment as evidenced by the observation that the mean molecular area of the porphyrin molecule was expanded at the air/subphase interface upon calcium binding (Figure 1). Recent studies have suggested that optimum structural adjustability of the template is an important function in the template/crystal interaction.[26e] Finally, but not the least, other functions, such as regulating the microenviron-

(61) (a) Taylor, M. G.; Simkiss, K.; Greaves, G. N.; Okazaki, M.; Mann, S. *Proc. R. Soc. London B* **1993**, *252*, 75−80. (b) Ziegler, A. *J. Struct. Biology* **1994**, *112*, 110−116.

(62) Addadi, L.; Weiner, S. In *Biomineralization: Chemical and biochemical perspectives*; Mann, S., Webb, J., Williams, R. J. P., Eds.; VCH: New York, 1989.

ment including CO_2 diffusion and local pH at the air/water interface and so on, though not technically addressable yet, are likely to have involved the porphyrin template. Nevertheless, as a whole, the semirigid array of carboxylate groups presented by the amphiphilic porphyrin monolayer apparently mimics the surface offered by the typical acidic glycopeptides.

The alignment of the crystalline film indicates that direct nucleation from solution is not the only pathway by which the structural information of the template can be transferred to the ensuing crystal. A template can control the orientation of a crystalline phase during a phase transformation process as well. Although our results support a multistep crystallization mechanism in calcium carbonate mineralization, they do not exclude the possibility of a direct nucleation process under some conditions.

The method we have demonstrated herein for the synthesis of calcium carbonate films not only provides a new access to forming inorganic thin films but also suggests that the cooperative interaction of controlling variables plays an important role in this biomimetic approach. The integration of such controlling factors as promotion, inhibition, and temperature has afforded a macroscopic-scale continuous thin film with a thickness about half a micrometer, which is comparable to the thickness of some biological calcite layers.[33,35,36] The method is simple, effective, and adaptable to other material systems. Specifically, the type and concentration of inhibitor should in principle be tunable to achieve an optimal balance between the promoting and inhibiting effects. The choices of inhibitor may also affect the orientation and even the crystalline phase of films.

Conclusion

We have synthesized macroscopic-scale continuous calcium carbonate thin films with a thickness ranging from 0.4 to 0.6 μm, using the synergistic interplay between a semirigid template and a soluble inhibitor, two of the crucial controls utilized in mineralization of organisms. The strategy applied provides a new perspective for biomimetic processing and thin film synthesis under mild conditions. The observation of an amorphous calcium carbonate precursor phase and its subsequent phase transformation into the crystalline phase provides direct evidence that the multistep-stage crystallization process is possible in a biomimetic environment. The structural correlation between the porphyrin template and the oriented crystal plane suggests that the organic matrix can regulate crystallization during the phase transformation as well.

Experimental Section

Film Preparation. The experimental setup for preparing the $CaCO_3$ thin film is illustrated in Scheme 1. The $Ca(HCO_3)_2$ subphase was prepared by bubbling CO_2 gas into Milli-Q deionized water in the presence of $CaCO_3$ for 2 h. Excess solid $CaCO_3$ was removed by filtering, and the filtrate was purged with CO_2 for another hour. The solution thus prepared had a calcium concentration of 8.5 mM as determined by EDTA titration. The freshly prepared $Ca(HCO_3)_2$ was immediately mixed with sodium polyacrylate (MW2,100, Fluka) solution to reach a final polymer concentration in the range of 10−40 ppm (μg/mL). Then, a porphyrin monolayer was deposited onto the surface of the subphase from a chloroform solution of the amphiphilic tricarboxyphenylporphyrin iron(III) μ-oxo dimers (**1**) we have previously described,[31] which served as a template for the $CaCO_3$ film formation. The surface pressure of the monolayer, which was measured with a Wilhelmy plate, reached the value that corresponded to a liquid-condensed or solid-state monolayer. In most cases, crystal dishes made of glass were used as the trough, which allowed convenient observations of the developing films with an optical microscope. The whole system was then left undisturbed at 22 °C while $CaCO_3$ formation took place through the slow, spontaneous loss of CO_2 from the $Ca(HCO_3)_2$ solution beneath the porphyrin monolayer. For the low-temperature experiments, the setup was kept in a "cold" room in which the temperature was maintained at 4 °C while all the rest of the experimental conditions remained the same.

Experiments performed in the absence of a porphyrin template, otherwise under identical conditions as above, for both room temperature and low temperature, were used as controls.

Film Characterization. In situ observations of the films were made with a Leica optical stereomicroscope equipped with cross polarizers in the transmission mode. Films were picked up either by dipping and subsequently withdrawing substrates through the surface film or by touching the film from above with substrates. The dipping technique enabled a view of the side that was facing the template while the latter method afforded a perspective of the flip side (i.e. the side facing the subphase) of the film. After being picked up, all the samples were naturally dried in the air and stored in desiccators at room temperature.

Films picked up on various substrates were examined by optical microscopy (OM), scanning electron microscopy (SEM), transmission electron microscopy (TEM), energy dispersion X-ray analysis (EDS), thermogravimetric analysis and differential scanning calorimetry (TGA/DSC), and infrared spectroscopy (IR). For OM studies, samples were picked up on a glass cover slip and checked with a Nikon compound microscope; for SEM studies, samples were picked up on either glass slides or silicon wafers, and then coated with Au/Pd and examined, with the operating voltage in the range of 5−10 keV, by Philips XL-30 Field Emission Gun (FEG) SEM; for TEM studies, samples were prepared by horizontal lift of the films through the air/subphase interface with holey carbon TEM grids to ensure a good contact between the samples and underlying carbon films. High-resolution TEM (HRTEM) and selected area diffraction (SAD) were obtained from the edges of fractured films with Philips CM-200 FEG-TEM (200 KV) and a low dose electron beam was used to avoid possible beam damage to the samples. For TGA/DSC studies, air-dried samples were heated at 10 deg C/min in a flow of air (14 mL/min) and analyzed in the STA (Simultaneous Thermal Analyzer) mode by the Rheometric Scientific STA-1500 system; for FTIR studies, samples were scanned at 4 cm^{-1} resolution in both mid-IR and far-IR regimes: films deposited on silver chloride pellets were scanned in the 4000−400 cm^{-1} range by a Nicolet-700 FTIR while samples pressed into KBr pellet were scanned in the range of 400−200 cm^{-1} by a Nicolet-800 FTIR instrument.

Synthesis of the amphiphilic tricarboxyphenylporphyrin iron (III) μ-oxo dimer was described previously.[63]

Acknowledgment. Financial support from National Science Foundation (IAA and JTG) and the National Institutes of Health (JTG, GM36298) and fellowship support for GX from the Princeton Materials Institute and Johnson & Johnson Co. are gratefully acknowledged. We also acknowledge Dr. Joydeep Lahiri, who first noticed the amorphous $CaCO_3$ phase, and Dr. Daniel M. Dabbs, for assistance with the TGA/DSC.

JA9819108

(63) Lahiri, J.; Fate, G. D.; Ungashe, S. B.; Groves, J. T. *J. Am. Chem. Soc.* **1996**, *118*, 2347.